

# StrainGain: Neck Strain Amplifies Head Pointing in VR

Guanlin Li<sup>\*</sup>  
Lancaster University

Florian Weidner<sup>†</sup>  
Glasgow University

Jinghui Hu<sup>¶</sup>  
Lancaster University

Anam Ahmad Khan<sup>‡</sup>  
Korea Advanced Institute of Science & Technology (KAIST)  
Hans Gellersen<sup>||</sup>  
Lancaster University  
Aarhus University

Haopeng Wang<sup>§</sup>  
Lancaster University



Figure 1: Strain-aware head pointing. Left: 1:1 mapping head pointing cannot reach the target, and neck strain occurred. Right: Neck strain drives the cursor and amplifies the pointing ray angle, enabling target acquisition.

## ABSTRACT

Head pointing is widely used in VR, but the standard 1:1 head-cursor mapping can result in large head movements, which may increase discomfort due to HMD weight and shifted balance. To address this, we introduce StrainGain, an ergonomics-first concept that adapts control-display (CD) gain according to estimated neck strain. We operationalise StrainGain with a lightweight regression model trained on an open-source neck EMG dataset. The predicted strain drives a cursor amplification. We evaluated the technique in a 2D Fitts' law-like head-pointing task against 1:1 mapping and HeadShift dynamic gain ( $N=18$ ). Results show that strain-aware amplification significantly reduces accumulated head movement relative to both baselines, with the strongest reduction at the largest amplitude ( $100^\circ$ ), accompanied by acceptable performance trade-offs. Overall, StrainGain demonstrates how physiological-state-informed gain control can reduce head movement during VR pointing, reframing gain adaptation as a mechanism for sustained comfort and well-being rather than performance alone.

**Index Terms:** Head pointing, Ergonomics, Head-Mounted Displays, Virtual Reality, Human Computer-Interaction, Neck Muscle Activity, Cursor

## 1 INTRODUCTION

A typical head-based interaction technique in VR is head pointing, where cursor direction is coupled to the head's forward vector. Conventional implementations often use an implicit 1:1 mapping: to place the cursor on a target, users must rotate their head until the target aligns with the centre of view. While simple and robust,

this coupling can require exaggerated head movements and may be uncomfortable, particularly when targets are distributed broadly in the scene or positioned vertically [20, 28, 31]. These ergonomic concerns are amplified by the fact that HMDs add mass and shift the effective centre of gravity of the head-neck system, increasing cervical spine (neck) loading and perceived discomfort during head movement and sustained postures [13, 29].

Prior work in pointing research shows that modifying the control-display (CD) gain, the mapping between physical input movement and cursor movement, can trade off speed, accuracy, and effort [22, 3, 23, 9, 17]. Recent VR-specific techniques, such as HeadShift [28], demonstrate that dynamic gain can reduce required head motion and improve ergonomics and error rate by allowing the cursor to move faster than the head during coarse movements. However, existing gain designs are typically driven by movement characteristics (speed/acceleration) [28] or task heuristics (e.g., proximity to targets) [10, 5], rather than the user's physical state, even though neck load and discomfort can vary substantially with pose and duration [20].

In this paper, we propose *StrainGain*, a concept that adapts CD gain based on estimated neck muscle strain during VR use. The core idea is straightforward: when the user is in a more demanding head posture, the system increases gain so that smaller head rotations produce larger cursor movements, thereby reducing additional neck motion needed to reach targets (Figure 1). Conversely, when posture is comfortable and strain is low, the strain-aware system can maintain a lower gain to support stable, precise cursor control. Essentially, this approach uses ergonomics as a first-class objective. Unlike most head-pointing work, which optimises speed/accuracy, *StrainGain* prioritises comfort and uses speed/accuracy as a constraint rather than the sole goal.

We evaluated the strain-aware cursor in a 2D Fitts-Law-like head pointing study, compared with HeadShift[28] and NoGain (1:1 mappings). The results show that strain-aware amplification can (1) reduce head movement during target acquisition and (2) preserve comparable pointing performance.

This work contributes: (i) the concept of *StrainGain*, linking control-display gain to predicted neck strain; (ii) an empirical evaluation of the resulting technique on pointing tasks representative of VR interaction demands, assessing both performance and comfort

\*e-mail: g.li12@lancaster.ac.uk

<sup>†</sup>e-mail: florian.weidner@glasgow.ac.uk

<sup>‡</sup>e-mail: anam.khan@kaist.ac.kr

<sup>§</sup>e-mail: h.wang73@lancaster.ac.uk

<sup>¶</sup>e-mail: j.hu23@lancaster.ac.uk

<sup>||</sup>e-mail: h.gellersen@lancaster.ac.uk

outcomes.

## 2 RELATED WORK

### 2.1 Neck ergonomics in HMDs

HMDs have been shown to lead to increased head movements (due to the decreased field of view of HMDs) and higher load on the muscles (due to the additional weight of HMDs) [1, 4, 26]. This has been observed in head pointing involving frequent movement [31] as well as in fixed head poses maintained over longer periods [14]. Other studies have reported neck muscle fatigue induced by head-worn equipment such as helmets and night vision goggles [27, 8]. Different head poses and holding time would significantly affect neck muscle activity in HMD [20, 18, 8]. Arm movement can also affect neck ergonomics, for example, with mid-air interactions in virtual reality (VR), causing discomfort in the neck and shoulder regions [15]. These studies motivate interaction design to mitigate neck strain.

### 2.2 Head pointing CD gain models

Prior work on head-pointing CD gain is grounded in the view that modifying the control–display relationship between physical input and cursor motion influences pointing behaviour. [3]. Early head-pointer studies showed that gain choice matters for head-controlled cursors (including that “best” settings for head input can differ from hand/mouse input), so gain is a design decision, not just a user preference [21]. Later work refined how gain should be defined for head pointing, suggesting some gain formulations are more stable across different viewing distances, which supports more consistent control in real use [24]. More recent systems increasingly treat gain as a way to support coarse-to-fine control: use a fast method to get near the target, then a slower/more precise method to finish. This appears in gaze+head combinations (coarse by gaze, refine by head) [2, 16] and in VR techniques like HeadShift that use dynamic gain to reduce required head motion while keeping the cursor comfortable to view in an HMD [28].

However, existing gain designs are typically driven by movement characteristics (speed/acceleration) or task heuristics (e.g., proximity to targets), rather than the user’s physical state. In this paper, we propose *StrainGain*, a concept that adapts CD gain based on estimated muscle strain or discomfort during VR use. *StrainGain* prioritised ergonomics as its primary objective, treating performance as a constraint rather than the sole goal.

## 3 NECK STRAIN AMPLIFIES HEAD POINTING IN VR

To facilitate our idea of *StrainGain*, we trained a lightweight Multi-Layer Perceptron (MLP) regression model with an open-source Neck electromyography (EMG) dataset [20], in order to predict real-time neck strain. The input to the model is a three-dimensional feature vector consisting of head posture (pitch, yaw) and head fixation time (t). The ground truth for each feature vector was the scaled sum of 6-channel EMG data. The  $R^2$  of the trained model is 0.72, indicating good performance on the regression tasks.

We design a model-based cursor amplification. The amount of *CursorAmplification* is defined as:

$$CursorAmplification = model(yawhead, pitchhead, 0) \times k \quad (1)$$

with  $model(yawhead, pitchhead, 0)$  as the model output and  $k$  is a constant scaling the model output.  $Yawhead$  and  $Pitchhead$  are head yaw and pitch. Note that the model input “time” is always set to 0 in this technique because we consider head movement not as a fixation.

We use *cursoramplification* to adjust the cursor position as follows, with  $Yaw_{offset}$  and  $Pitch_{offset}$  being extra pitch and yaw degrees related to head orientation:

$$\begin{aligned} Yaw_{offset} &= \cos(\alpha) \times cursoramplification, \\ Pitch_{offset} &= \sin(\alpha) \times cursoramplification, \\ \text{with } \alpha &= \text{atan2}(pitchhead, yawhead). \end{aligned} \quad (2)$$

With a 1:1 mapping,  $Yaw_{offset}$  and  $Pitch_{offset}$  always equal 0; the cursor position is the same as the head orientation. To limit the cursor amplification and avoid the cursor being out of the user’s field of view, we clamp the value between 0 and the maximum amplification. A previous study on eye-head coordination in HMD shows a comfortable eye-in-head angle of around 15 to 25 degrees, depending on direction [25]. Thus, we set the maximum amplification in the upper direction to 15°, while in other directions to 25°. With that, the  $Yaw_{offset}$  and  $Pitch_{offset}$  are never more than the maximum amplification in their specific direction. To further demonstrate the concept of *StrainGain*, we fine-tune the parameter to enhance ergonomics and set  $k$  in Equation 1 to 30.

## 4 USER STUDY EVALUATION

### 4.1 Task Description

We compare our ModelGain cursor with HeadShift [28] and No-Gain (1:1 mappings) cursor in a Fitts-Law-like task. We opted for a Fitts-Law-like task to get a deeper insight into behaviour on larger target amplitudes beyond the field of view ( $>40^\circ$ ), different from the typical Fitt’s Law setup [6]. We asked participants to point at targets via head pointing and confirm selection via the controller trigger button. We had 11 targets arranged in a circle [28]. Following a sequence, participants must select 23 times to complete a round. We discarded the first trial in each round. In the task, we varied amplitude (40°, 70°, and 100°), target size (2° and 4° diameter), and techniques (ModelGain, HeadShift, and NoGain).

### 4.2 Procedure

Upon arrival, we briefed participants about the experiment, and they filled out consent forms and a demographic questionnaire. Participants were seated and fitted with the HMD. After that, the participant experienced the pointing and selection task. We compare our techniques (ModelGain) against HeadShift [28] and a 1:1 mapping (no gain). The sequence of techniques counterbalanced the effect of positions, ensuring each technique appears equally often in 1st/2nd/3rd place. Before starting the study, we explained the task, and the participants practised until they were comfortable. After each technique, they removed the headset to complete questionnaires. Breaks were offered between tasks. The study was approved by the institutional ethics board, took around 30 minutes, and participants were compensated with 5 GBP.

During the study, we required participants to sit on a stationary chair and keep their lower limbs stationary. We measure the head angle related to the world by the headset.

### 4.3 Measures

We measure completion time, cumulative head movement (in degrees), throughput (in ISO 9241-411 standard [6]), and error rate. In addition, we ask participants to fill out the RAW NASA-TLX [11] and rate preference and comfort level on a 7-point Likert scale after each technique. Specifically, we ask “How comfortable is the technique?” (1 = “not at all”, 7 = “very comfortable”) and “How much do you like the technique?” (1 = “not at all”, 7 = “very much like it”).

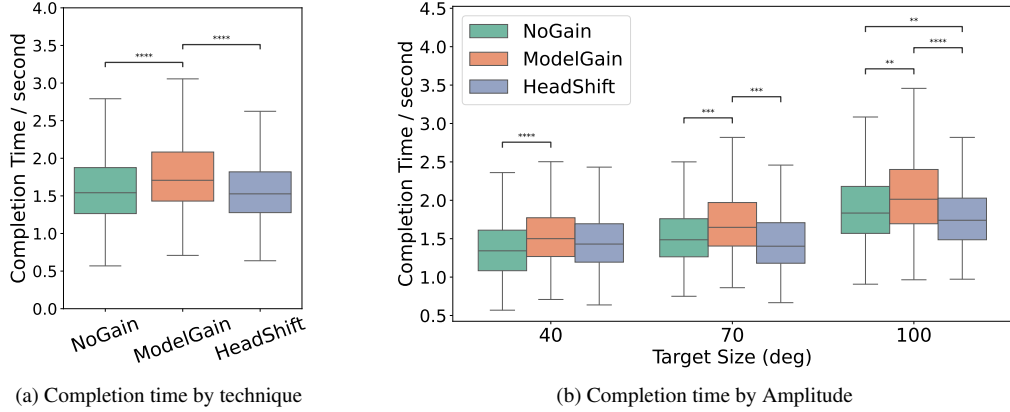


Figure 2: Mean completion time. Each box indicates the interquartile range (25th-75th percentile), with the horizontal line marking the median. The whiskers extend to  $1.5 \times$  interquartile range.

#### 4.4 Apparatus

We implemented the scenarios and the individual techniques with Unity 2022.3.49f1. We used a Meta Quest 3 VR headset for the study, with  $146^\circ$  diagonal rendered FOV,  $2064 \times 2208$  per-eye pixels resolution, and 72 Hz refresh rate on a computer with an Intel Core i7-12700 CPU, 16 GB RAM, and an NVIDIA GeForce RTX 3070 Ti GPU. This tests the model’s utility across headsets, as data was collected using the HTC Vive Pro Eye.

#### 4.5 Sample

We recruited 18 participants (11 female, 7 male) from a local university, with an average age of 29.4 years ( $SD = 8.6$ , range 22–53). None reported neck, shoulder, or dermatological issues. Around 88% had limited VR experience: 3 had none, 12 used it rarely, and 1 used it monthly.

#### 4.6 Results

We analysed data with a three-way repeated measures ANOVA ( $\alpha = .05$ ) with Technique, Amplitude, and TargetSize as independent variables. When Mauchly’s test indicated a violation of sphericity, we applied Greenhouse-Geisser corrections. We used the Shapiro-Wilk test and QQ plots to assess normality and applied the Aligned Rank Transform (ART) when normality was violated. We performed Bonferroni-corrected post-hoc tests where applicable. We reported effect sizes using general eta squared ( $\eta^2$ ) for interactions and main effects and Cohen’s d for post-hoc tests. We discarded trials with completion time beyond three standard deviations from the mean of each condition as outliers (36 trials, 0.51%). We analysed NASA-TLX, Comfort, and Preference data using Wilcoxon signed-rank tests and report effect sizes using rank-biserial correlations ( $r$ ).

##### 4.6.1 Completion Time

We found a significant two-way interaction between Technique  $\times$  Amplitude ( $F(4,68) = 13.3$ ,  $p < 0.001$ ,  $\eta^2 = 0.031$ , see Figure 2b). Post-hoc pairwise comparison showed that ModelGain’s completion time was higher than NoGain in all amplitudes ( $p \leq 0.002$ ) and higher than HeadShift in  $70^\circ$  and  $100^\circ$  amplitudes ( $p < 0.001$ ). HeadShift was significantly faster than NoGain in  $100^\circ$  ( $p = 0.003$ ).

We found a significant two-way interaction between Technique  $\times$  targetSize ( $F(2,34) = 6.23$ ,  $p = 0.005$ ,  $\eta^2 = 0.009$ ). Post-hoc pairwise comparison showed that ModelGain’s completion time was higher than NoGain in both target size ( $p \leq 0.003$ ) and higher than HeadShift in both target size ( $p < 0.001$ ).

We found a significant main effect of Technique ( $F(2,34) = 24$ ,  $p = .12$ ,  $\eta^2 = 0.128$ ), Figure 2a). Post-hoc pairwise comparison showed ModelGain’s completion time was higher than NoGain ( $p < 0.001$ ) and HeadShift ( $p < 0.001$ ).

We found significant main effects of Amplitudes ( $F(2,34) = 279$ ,  $p < 0.001$ ,  $\eta^2 = 0.38$ ) and target size ( $F(1,17) = 274$ ,  $p < 0.001$ ,  $\eta^2 = 0.39$ ). Post-hoc pairwise comparison shows significant differences between all three amplitudes ( $p < 0.001$ ), where the amplitude of  $100^\circ$  needs longer completion time than  $70^\circ$  and  $40^\circ$  and  $70^\circ$  longer than  $40^\circ$ . Post-hoc pairwise comparison shows target size of  $2^\circ$  higher than  $4^\circ$  ( $p \leq 0.001$ ). There were no other main or interaction effects ( $p \geq 0.54$ ).

##### 4.6.2 Error Rate

We found a significant two-way interaction between Technique  $\times$  TargetSize ( $F(2,289) = 3.58$ ,  $p = 0.029$ ,  $\eta^2 = 0.024$ , see Figure 3b), where post-hoc pairwise comparison showed HeadShift has a lower error rate in target size of 2 compared with ModelGain ( $p \leq 0.001$ ) and NoGain ( $p < 0.001$ ). NoGain has a lower error rate in the target size of 4 compared with ModelGain ( $p = 0.007$ ).

We found a significant main effect of Technique ( $F(2,289) = 16$ ,  $p < 0.001$ ,  $\eta^2 = 0.10$ ), see Figure 3a). Post-hoc pairwise comparison showed the ModelGain error rate was higher than HeadShift ( $p < 0.001$ ) and had no significant difference when compared with NoGain. Post-hoc comparisons also showed a significant difference between NoGain and HeadShift ( $p = 0.002$ ), where the NoGain error rate is higher than HeadShift’s.

We found significant main effects of Amplitudes ( $F(2,289) = 3$ ,  $p = 0.04$ ,  $\eta^2 = 0.02$ ) and target size ( $F(1,289) = 43$ ,  $p < 0.001$ ,  $\eta^2 = 0.12$ ). Post-hoc pairwise comparison shows no significant differences between the three amplitudes ( $p \geq 0.07$ ), but shows the target size of  $2^\circ$  has a higher error rate than  $4^\circ$  ( $p < 0.001$ ).

There were no other main or interaction effects ( $p \geq 0.49$ ).

##### 4.6.3 Throughput

We found a significant two-way interaction between Technique  $\times$  target size ( $F(2,34) = 3.38$ ,  $p = 0.046$ ,  $\eta^2 = 0.016$ ), where post-hoc pairwise comparison showed NoGain is higher than the ModelGain ( $p < 0.001$ ) and HeadShift ( $p < 0.001$ ) in target size of 2. The throughput of ModelGain is higher than HeadShift’s ( $p = 0.006$ ) in the target size of 2. In the target size of 4, NoGain and ModelGain are higher than HeadShift with both  $p < 0.001$ .

Besides, we found a significant two-way interaction between Technique  $\times$  Amplitude ( $F(4,68) = 15$ ,  $p < 0.001$ ,  $\eta^2 = 0.148$ , see Figure 4b). Post-hoc pairwise comparison revealed NoGain higher

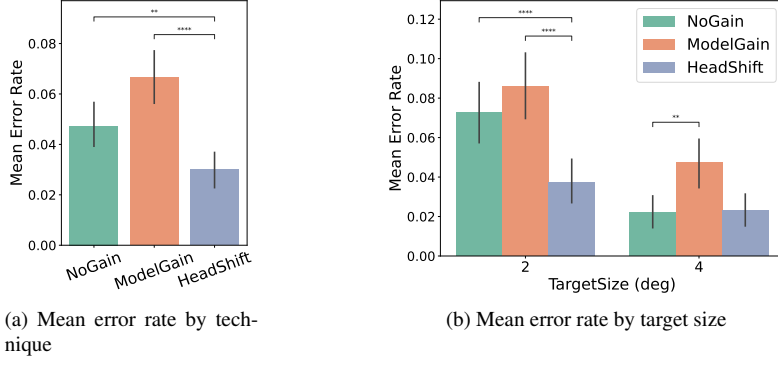


Figure 3: Mean error rate with 95%CI.

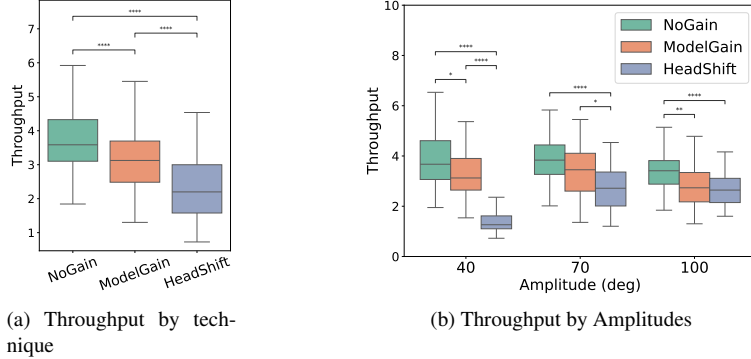


Figure 4: Task performance during the pointing and selection task. Each box indicates the interquartile range (25th-75th percentile), with the horizontal line marking the median. The whiskers extend to  $1.5 \times$  interquartile range, and individual points represent outliers.

than HeadShift in all three amplitudes (all  $p < 0.001$ ), and NoGain higher than ModelGain in both amplitudes of  $40^\circ$  ( $p = 0.048$ ) and  $100^\circ$  ( $p = 0.006$ ). ModelGain higher than HeadShift in amplitude of  $40^\circ$  ( $p < 0.001$ ) and  $70^\circ$  ( $p = 0.044$ ).

We found a significant main effect of Technique ( $F(2,34) = 48$ ,  $p = 0.12$ ,  $\eta^2 = 0.32$ , Figure 4a). Post-hoc pairwise comparison revealed significant differences between the 3 techniques. Specifically, the throughput of NoGain is higher than the ModelGain ( $p < 0.001$ ) and HeadShift ( $p < 0.001$ ). At the same time, the throughput of ModelGain is higher than HeadShift's ( $p < 0.001$ ).

Additionally, we found significant main effects of Amplitudes ( $F(2,34) = 15.9$ ,  $p < 0.001$ ,  $\eta^2 = 0.056$ ) and target size ( $F(1,17) = 60$ ,  $p < 0.001$ ,  $\eta^2 = 0.094$ ). Post-hoc pairwise comparison shows significant differences between the amplitude pairs of ( $40^\circ$ ,  $70^\circ$ ) and ( $70^\circ$ ,  $100^\circ$ ) (all  $p < 0.001$ ), where  $70^\circ$  is higher than  $40^\circ$  and  $70^\circ$  is higher than  $100^\circ$ . It also shows significance in the two target sizes ( $p < 0.001$ ). There were no other significant effects ( $p \geq 0.9$ ).

#### 4.6.4 Accumulated Head Movement

We found a significant two-way interaction between Technique  $\times$  Amplitude ( $F(2.33,39.6) = 106.7$ ,  $p = 0.485$ ,  $\eta^2 = 0.829$ , Figure 5b). Post-hoc pairwise comparison showed that our technique and HeadShift required less head movement than NoGain for all amplitudes (all  $p < 0.001$ ). Post-hoc comparison also revealed that our model reduces head movement in  $100^\circ$  amplitudes ( $p < 0.001$ ).

We found significant two-way interaction between Technique  $\times$  target size ( $F(2,289) = 12.5$ ,  $p < 0.001$ ,  $\eta^2 = 0.08$ ), where post-hoc comparison shows NoGain in  $4^\circ$  target size have longer head movement than its in  $2^\circ$  size ( $p < 0.001$ ). Other results show similar

patterns to the main effect of Technique, with all  $p < 0.001$ .

Besides, we found a significant main effect of Technique ( $F(2,289) = 445$ ,  $p < 0.001$ ,  $\eta^2 = 0.75$ , see Figure 5a), where post-hoc comparison revealed that head movement of NoGain is higher than both ModelGain ( $p < 0.001$ ) and HeadShift ( $p < 0.001$ ). Head movement of HeadShift is also higher than ModelGain ( $p < 0.001$ ).

We found significant main effects of Amplitudes ( $F(2,289) = 532$ ,  $p < 0.001$ ,  $\eta^2 = 0.78$ ) and target size ( $F(1,289) = 13.7$ ,  $p < 0.001$ ,  $\eta^2 = 0.045$ ). Post-hoc pairwise comparison shows all significant differences between the three amplitudes ( $p < 0.001$ ) and between both target sizes ( $p < 0.001$ ).  $100^\circ$  has a higher head move than  $70^\circ$  and  $40^\circ$ . The amplitude of  $70^\circ$  is higher than  $40^\circ$ . The target size of  $2^\circ$  has a higher head move than  $4^\circ$ . There were no other main or interaction effects ( $p > 0.18$ ).

#### 4.6.5 Endpoint Distribution

Figure 6 shows the endpoint distribution of all three techniques in all amplitudes. The endpoint is the head pose (pitch, yaw) when pressing the selection button in a trial. ModelGain and NoGain cluster into several small groups, while HeadShift spreads and varies in different locations, especially in  $40^\circ$  target amplitudes.

To quantify the degree of clustering in the endpoint data, we used the Hopkins statistic [12]. We found that HeadShift (Hopkins = 0.803) exhibits less clustering compared to ModelGain (Hopkins = 0.960) and NoGain (Hopkins = 0.965).

#### 4.6.6 Subjective Metrics

We did not find significant differences in Raw NASA-TLX, Preference, and Comfort level results (all  $p > 0.10$ ).

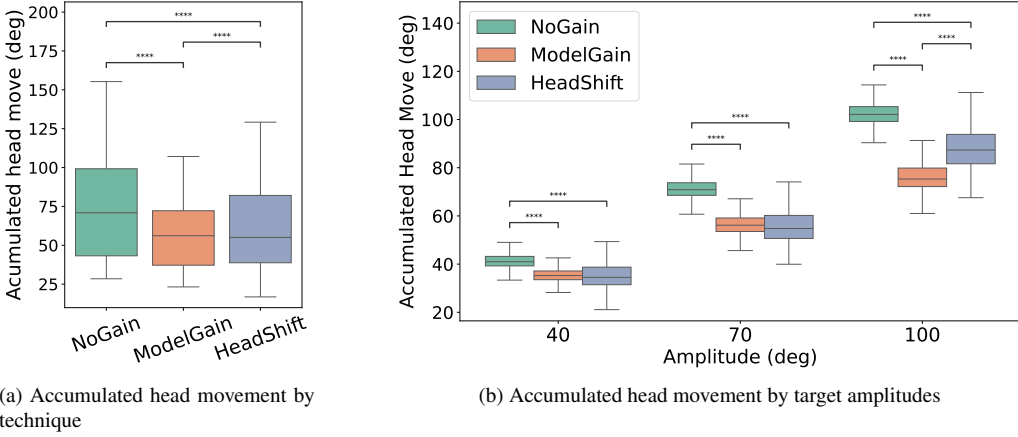


Figure 5: Accumulated head movement by amplitude

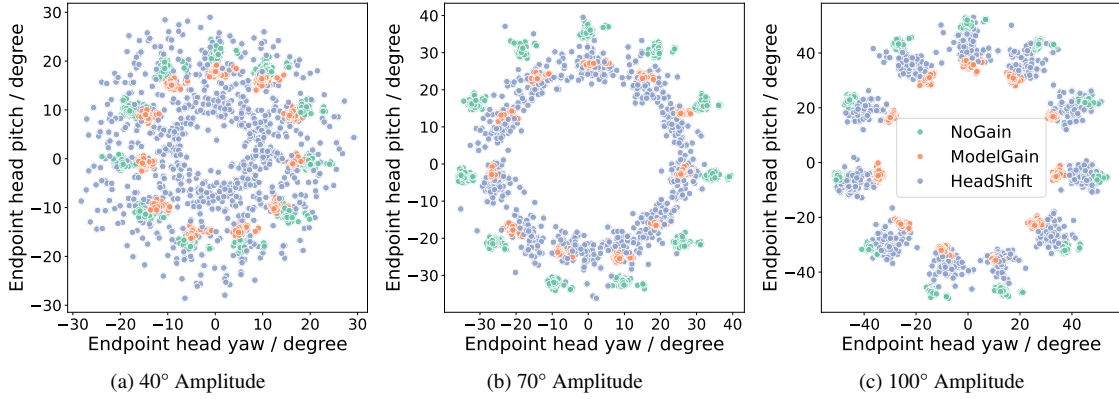


Figure 6: End Point Distribution for 40°, 70° and 100° Amplitudes. The endpoint is the head pose recorded when the selection button is pressed.

## 5 DISCUSSION

### 5.1 Techniques performance

Our results show that the ModelGain can reduce head movement compared to both HeadShift and the baseline 1:1 mapping. In particular, ModelGain further lowered accumulated head movement at large amplitudes (100°), which indicates that adapting cursor gain based on predicted muscle strain can offer ergonomic advantages beyond approaches that only consider head kinematics. The endpoint distributions support this: selections with ModelGain were more clustered, stabilising the amount of head movement. At the same time, the ModelGain cursor reduces extreme head rotations at a cost to performance. Completion times with ModelGain were slower than both HeadShift and the baseline, and error rates were higher than HeadShift (but not different from 1:1).

*StrainGain* optimises ergonomics by design, using performance as a constraint rather than the sole goal. To further demonstrate the concept of *StrainGain*, we fine-tune the parameter to enhance ergonomics. The balance between ergonomics and performance can be adjusted as needed.

### 5.2 Prioritising ergonomics over performance

Head pointing performance (e.g., Fitts' law speed/accuracy) can reach a “good enough” level quickly, especially when targets of moderate size are used. But neck comfort becomes the limiting fac-

tor as session time, target distribution, and vertical reach increase [20, 19]. Over time, neck discomfort may degrade performance [30]. As users tire, they adopt compensatory strategies (e.g., smaller neck motions, increased trunk variability) [30, 7], potentially increasing errors, time, and frustration. Therefore, prioritising ergonomics is not only a wellbeing goal; it directly supports sustained effectiveness and enables interface layouts that would otherwise be impractical with head pointing alone.

## 6 CONCLUSION

We introduced StrainGain, an ergonomics-first approach that adapts head-pointing control-display gain based on predicted neck strain, allowing users to reach targets with less head rotation as posture becomes more demanding. The study results show that strain-aware techniques can significantly reduce accumulated head movement, with certain trade-offs in accuracy and speed. StrainGain demonstrates how physiological-state-informed gain control can reduce head movement during VR pointing. Besides, the study proved the feasibility of prioritising ergonomics in pointing techniques and discussed its value in prolonged immersion. Future work can apply the *StrainGain* concept to other modalities (arm fatigue in mid-air interaction) to better balance comfort and efficiency in everyday VR interaction.

## REFERENCES

- [1] A. N. Astrologo, S. Nano, E. M. Klemm, S. J. Shefelbine, and J. T. Dennerlein. Determining the effects of AR/VR HMD design parameters (mass and inertia) on cervical spine joint torques. *Applied Ergonomics*, 116:104183, Apr. 2024. doi: 10.1016/j.apergo.2023.104183 2
- [2] J. Borah. Investigation of Eye and Head Controlled Cursor Positioning Techniques. Sept. 1995. Number: ALCFTR19950018. 2
- [3] G. Casiez, D. Vogel, R. Balakrishnan, and A. Cockburn. The Impact of Control-Display Gain on User Performance in Pointing Tasks. *Human-Computer Interaction*, 23(3):215–250, Aug. 2008. Publisher: Taylor & Francis eprint: <https://www.tandfonline.com/doi/pdf/10.1080/07370020802278163> 1, 2 doi: 10.1080/07370020802278163 1, 2
- [4] Y. Chen and Z. Wu. A review on ergonomics evaluations of virtual reality. *Work*, 74(3):831–841, Jan. 2023. doi: 10.3233/WOR-205232 2
- [5] W. Delamare, M. Daniel, and K. Hasan. MultiFingerBubble: A 3D Bubble Cursor Variation for Dense Environments. In *Extended Abstracts of the 2022 CHI Conference on Human Factors in Computing Systems*, CHI EA '22, pp. 1–6. Association for Computing Machinery, New York, NY, USA, 2022. doi: 10.1145/3491101.3519692 1
- [6] I. O. for Standardisation. ISO 9241-411:2012 Ergonomics of human-system interaction — Part 411: Evaluation methods for the design of physical input devices. Standard ISO 9241-411:2012, International Organization for Standardization, Geneva, Switzerland, 2012. 2
- [7] J. R. Fuller, J. Fung, and J. N. Côté. Posture-movement responses to stance perturbations and upper limb fatigue during a repetitive pointing task. *Human movement science*, 32(4):618–632, Aug. 2013. doi: 10.1016/j.humov.2013.03.002 5
- [8] H. Gallagher, E. Caldwell, and C. ALbery. Neck Muscle Fatigue Resulting from Prolonged Wear of Weighted Helmets. Jan. 2008. 2
- [9] L. Gallo and A. Minutolo. Design and comparative evaluation of Smoothed Pointing: A velocity-oriented remote pointing enhancement technique. *International Journal of Human-Computer Studies*, 70(4):287–300, Apr. 2012. doi: 10.1016/j.ijhcs.2011.12.001 1
- [10] T. Grossman and R. Balakrishnan. The bubble cursor: enhancing target acquisition by dynamic resizing of the cursor's activation area. In *Proceedings of the SIGCHI Conference on Human Factors in Computing Systems*, CHI '05, pp. 281–290. Association for Computing Machinery, New York, NY, USA, 2005. doi: 10.1145/1054972.1055012 1
- [11] S. G. Hart. NASA-Task Load Index (NASA-TLX); 20 Years Later. *Proceedings of the Human Factors and Ergonomics Society Annual Meeting*, Oct. 2006. Publisher: SAGE PublicationsSage CA: Los Angeles, CA. doi: 10.1177/154193120605000909 2
- [12] B. Hopkins and J. G. Skellam. A New Method for determining the Type of Distribution of Plant Individuals. *Annals of Botany*, 18(70):213–227, 1954. Publisher: Oxford University Press. 4
- [13] K. Ito, M. Tada, H. Ujike, and K. Hyodo. Effects of the Weight and Balance of Head-Mounted Displays on Physical Load. *Applied Sciences*, 11(15):6802, Jan. 2021. doi: 10.3390/app11156802 1
- [14] E. Kim and G. Shin. Head Rotation and Muscle Activity When Conducting Document Editing Tasks with a Head-Mounted Display. *Proceedings of the Human Factors and Ergonomics Society Annual Meeting*, 62(1):952–955, Sept. 2018. doi: 10.1177/1541931218621219 2
- [15] J. H. Kim, H. Ari, C. Madasu, and J. Hwang. Evaluation of the biomechanical stress in the neck and shoulders during augmented reality interactions. *Applied Ergonomics*, 88:103175, Oct. 2020. doi: 10.1016/j.apergo.2020.103175 2
- [16] A. Kurauchi, W. Feng, C. Morimoto, and M. Betke. HMAGIC: head movement and gaze input cascaded pointing. In *Proceedings of the 8th ACM International Conference on PErvasive Technologies Related to Assistive Environments*, PETRA '15, pp. 1–4. Association for Computing Machinery, New York, NY, USA, 2015. doi: 10.1145/2769493 .2769550 2
- [17] W. A. König, J. Gerken, S. Dierdorf, and H. Reiterer. Adaptive Pointing – Design and Evaluation of a Precision Enhancing Technique for Absolute Pointing Devices. In T. Gross, J. Gulliksen, P. Kotzé, L. Oestreicher, P. Palanque, R. O. Prates, and M. Winckler, eds., *Human-Computer Interaction – INTERACT 2009*, pp. 658–671. Springer, Berlin, Heidelberg, 2009. doi: 10.1007/978-3-642-03655-2\_73 1
- [18] D. H. Lee and S. K. Han. Effects of Watching Virtual Reality and 360° Videos on Erector Spinae and Upper Trapezius Muscle Fatigue and Cervical Flexion-Extension Angle. *Journal of the Korean Society for Precision Engineering*, 35(11):1107–1114, Nov. 2018. doi: 10.7736/KSPE.2018.35.11.1107 2
- [19] G. Li. [DC] Neck Muscles in Head-Mounted Displays Interaction. In *2025 IEEE Conference on Virtual Reality and 3D User Interfaces Abstracts and Workshops (VRW)*, pp. 1574–1575, Mar. 2025. doi: 10.1109/VRW66409.2025.00432 5
- [20] G. Li, F. Weidner, J. Hu, and H. Gellersen. Quantifying neck muscle activity during head fixation in VR. *Frontiers in Virtual Reality*, 6, Nov. 2025. Publisher: Frontiers. doi: 10.3389/fvrir.2025.1682866 1, 2, 5
- [21] M. L. LIN, R. G. RADWIN, and G. C. VANDERHEIDEN. Gain effects on performance using a head-controlled computer input device. *Ergonomics*, 35(2):159–175, Feb. 1992. Publisher: Taylor & Francis eprint: <https://doi.org/10.1080/00140139208967804> 2
- [22] D. E. Meyer, R. A. Abrams, S. Kornblum, C. E. Wright, and J. E. Keith Smith. Optimality in human motor performance: Ideal control of rapid aimed movements. *Psychological Review*, 95(3):340–370, 1988. Place: US Publisher: American Psychological Association. doi: 10.1037/0033-295X.95.3.340 1
- [23] M. Nancel, O. Chapuis, E. Pietriga, X.-D. Yang, P. P. Irani, and M. Beaudouin-Lafon. High-precision pointing on large wall displays using small handheld devices. In *Proceedings of the SIGCHI Conference on Human Factors in Computing Systems*, pp. 831–840. ACM, Paris France, Apr. 2013. doi: 10.1145/2470654.2470773 1
- [24] J. A. Schaab, R. G. Radwin, G. C. Vanderheiden, and P. K. Hansen. A Comparison of Two Control-Display Gain Measures for Head-Controlled Computer Input Devices. *Human Factors*, 38(3):390–403, Sept. 1996. Publisher: SAGE Publications Inc. doi: 10.1518/001872096778702042 2
- [25] L. Sidenmark and H. Gellersen. Eye, Head and Torso Coordination During Gaze Shifts in Virtual Reality. *ACM Transactions on Computer-Human Interaction*, 27(1):1–40, Jan. 2020. doi: 10.1145/3361218 2
- [26] A. D. Souchet, D. Lourdeaux, A. Pagani, and L. Rebenitsch. A narrative review of immersive virtual reality's ergonomics and risks at the workplace: cybersickness, visual fatigue, muscular fatigue, acute stress, and mental overload. *Virtual Reality*, July 2022. doi: 10.1007/s10055-022-00672-0 2
- [27] M. Thuresson, B. Äng, J. Linder, and K. Harms-Ringdahl. Mechanical load and EMG activity in the neck induced by different head-worn equipment and neck postures. *International Journal of Industrial Ergonomics*, 35(1):13–18, Jan. 2005. doi: 10.1016/j.ergon.2004.06.008 2
- [28] H. Wang, L. Sidenmark, F. Weidner, J. Newn, and H. Gellersen. Head-Shift: Head Pointing with Dynamic Control-Display Gain. *ACM Trans. Comput.-Hum. Interact.*, Aug. 2024. Just Accepted. doi: 10.1145/3689434 1, 2
- [29] Y. Yan, K. Chen, Y. Xie, Y. Song, and Y. Liu. The Effects of Weight on Comfort of Virtual Reality Devices. In F. Rebelo and M. M. Soares, eds., *Advances in Ergonomics in Design*, pp. 239–248. Springer International Publishing, Cham, 2019. doi: 10.1007/978-3-319-94706-8\_27 1
- [30] C. Yang, S. Leitkam, and J. N. Côté. Effects of different fatigue locations on upper body kinematics and inter-joint coordination in a repetitive pointing task. *PLOS ONE*, 14(12):e0227247, Dec. 2019. Publisher: Public Library of Science. doi: 10.1371/journal.pone.0227247 5
- [31] Y. Zhang, K. Chen, and Q. Sun. Toward Optimized VR/AR Ergonomics: Modeling and Predicting User Neck Muscle Contraction. In *Special Interest Group on Computer Graphics and Interactive Techniques Conference Conference Proceedings*, pp. 1–12. ACM, Los Angeles CA USA, July 2023. doi: 10.1145/3588432.3591495 1, 2